Journal of the Nivar

Homepage: https://nivar.irimo.ir

Volume 50, Special Issue, Spring and Summer 2026, P. 21-43

(Research Article)

Analysis of Climate Scenarios and Wheat Water Productivity in Khorasan Razavi Province with a Sustainable Approach

Dehghani, T[1] | Liaghat, A[2]* | Nazari, B[3]

[1.] PhD Candidate in Irrigation and Drainage, Department of Irrigation and Reclamation, Faculty of Agriculture and Natural Resource, University of Tehran, Karaj, Iran.
[2.] Professor, Department of Irrigation and Reclamation, Faculty of Agriculture and Natural Resource, University of Tehran, Karaj, Iran.
[3.] Associate Professor, Department of Irrigation and Reclamation, Faculty of Agriculture and Natural Resource, University of Tehran, Karaj, Iran; Faculty Member at Imam Khomeini International University, Qazvin, Iran.

Corresponding Author E-mail: aliaghat@ut.ac.ir

(Received: 02 Jan 2025, Revised: 14 Jun 2026, Accepted: 17 Jun 2026, Published online: 17 Jun 2026)

Abstract
Climate change, as one of the major challenges of the 21st century, has widespread impacts on agricultural production and food security. In this study, LARS-WG 8 models were used to generate climate data and AquaCrop 7.1 to simulate wheat yield in Khorasan Razavi Province. the effects of different greenhouse gas emission scenarios (SSP1-2.6, SSP2-4.5, and SSP5-8.5) were assessed towards 2040. The results showed that the LARS WG model performs reasonably well in generating average precipitation and temperature, but shows limitations in representing temperature variability and fluctuations. According to the results the average temperature at Sabzevar, Quchan, and Torbat-e Jam stations will increase the most in the SSP5-8.5 scenario; for example, the average temperature in Quchan will increase from 12.7 degrees in the period 2010-2024 to 14.1°C in SSP5-8.5. Future precipitation is expected to increase by 11–38 %, while reference evapotranspiration (ET_0) may decline by 8–32%. The average grain yield of wheat in Khorasan Razavi Province is projected to increase by about 7 to 13% across scenarios. Water productivity (WP) has also projected to rise from 1.7 in 2023 to 1.9 and 2.0 under different scenarios.
The findings of this study indicate that climate change in the 2040 horizon could, under some conditions, lead to increased yield and water productivity of wheat in Khorasan Razavi Province. However, these increases will only be sustainable if they are accompanied by smart water resource management, selection of resistant varieties, and adaptive policies to address the risks of warming, changing rainfall patterns, and the spread of pests and diseases. Therefore, although the short-term results are promising, from a sustainability perspective, a comprehensive and forward-looking approach is required to ensure food security and agricultural resilience in the region.

Keywords: AquaCrop, Agro-climatic Modeling, Climate Change, LARS WG, Resilience, SSPs Scenarios

Cite this article: Dehghani,T , Liaghat,A and Nazari,B . (2026). Analysis of Climate Scenarios and Wheat Water Productivity in Khorasan Razavi Province with a Sustainability Approach. Journal of the Nivar, Special Issue, 21-43. DOI: https://doi.org/10.30467/nivar.2026.570227.1365

E-mail: (1) tahmine.dehghani@ut.ac.ir (3) bnazari@ut.ac.ir

Publisher: Iran Meteorological Organization
DOI: https://doi.org/10.30467/nivar.2026.570227.1365

Print ISSN: 1735-0565
Online ISSN: 2645-3347

1. Introduction

Climate change, as one of the critical challenges of the 21st century, has profound implications for sustainable agricultural production and global food security (Bouteska et al. 2024). Rising temperatures, altered precipitation patterns, and the intensified extreme climate events directly affect water resources and crop yields (Xiao et al. 2020). Wheat, as a strategic staple and the primary source of caloric intake in Iran, holds particular importance in studies related to climate change and water resources management. Khorasan Razavi Province, with a significant share in the country's wheat production (Agricultural Yearbook, 2023), is particularly vulnerable to climate change impacts owing to its geographical position and semi-arid climate (Aalijahan and Khosravichenar, 2021). Analyzing future climate scenarios and assessing wheat water productivity in this province can provide a valuable insight for policy-making and sustainable management of water and soil resources. In this context, the application of climate and crop growth simulation models is a powerful tool for prediction and decision-making. The LARS-WG[1] model, as a statistical generator of climate data, enables the simulation of key variables such as temperature and precipitation under diverse climate change scenarios (Dheyaa et al, 2024). Generating climate data for 2040 with this model will provide a robust foundation for evaluating the possible effects of climate change on agriculture in the region.

On the other hand, the AquaCrop model developed by the Food and Agriculture Organization of the United Nations (FAO) is a reliable and widely validated tool for simulating crop yield under different management and climate conditions (Dehghani et al, 2026). Combining the data generated by LARS-WG 8 with AquaCrop 7.1 simulations enables a comprehensive analysis of the impact of climate change on wheat yield and water productivity in Khorasan Razavi Province (Ahmadi et al. 2024; Dehghani et al, 2026). This integrated approach not enhances understanding of the climate–yield nexus, but also provides a scientific basis for developing adaptive management strategies aimed at improving water productivity, mitigating climate-related risks, and strengthening food security at both regional and national scales.

Raoufi and Soufizadeh. (2020) employed the AquaCrop model to investigate the impact of climate change on the yield performance of different rice genotypes in northern Iran. Three improved varieties and one local genotype were simulated under different RCP scenarios, temperature increments (+1 to +4 C), and rainfall variations (±20%) across two time horizons, representing the near and far future. The results indicated that improved cultivars exhibited greater resilience compared to the local genotype, and that elevated CO_2 concentrations combined with higher temperatures frequently enhanced yield. Similarly, Li et al. (2024) applied the AquaCrop model to examine the combined effects of climate change and planting date on cotton yield in major cotton producing regions in China. Future climate data from 27 global circulation models (CMIP6) were simulated under SSP2-4.5 and SSP5-8.5 scenarios for the 2040s and 2080s. Findings revealed that cotton yield would increase by an average of 10–28% in the future, while early planting (March 31) resulted in approximately 5% higher yield compared to late planting (May 10).

Ahmadi et al. (2024) applied the AquaCrop model to simulate wheat yield in the Qazvin plain under climate change conditions. Future climate data were generated using the LARS WG model and incorporated as model input. The results indicated that the maximum wheat yield in the base period (1986–2015) was 8.59 t/ha, whereas the maximum predicted yields in the periods 2040, 2060, 2080 and 2100 were 9.86, 10.50, 11.78 and 12.29 t/ha, respectively. The minimum wheat yield in the base period was 6.96 t/ha, while the minimum predicted yields in the studied periods were 8.22, 8.56, 8.40 and 8.28 t/ha, respectively. Similarly, Sedhai et al. (2023) utilized AquaCrop to examine the impact of climate change on water demand and wheat yield in the Madabar Irrigation Project, Chitwan, Nepal. Future climate data from the CMIP6 suite and five global models were used under two scenarios (SSP245 and SSP585) for three time periods in the near, medium and far future. The results showed that wheat yield in the SSP245 scenarios would increase by 13 to 29% under rainfed conditions and by 10 to 17% under irrigated conditions. Also, the net irrigation demand was projected to decrease by approximately 130 relative to the baseline period, indicating a change in water use patterns in the future.

In the Tensift region of Morocco, Bouras et al. (2019) employed Med-CORDEX data in combination with the AquaCrop model to assess the impacts of climate change on wheat production. Their findings indicated that rising temperatures

[1] Long Ashton Research Station Weather Generator

could shorten the wheat growth cycle by up to 50 days. Without accounting for the effect of CO_2 fertilization, wheat yields were projected to decline by 7–30%, whereas accounting for CO_2 fertilization led to yield increases of 7% and 13% by mid-century under RCP4.5 and RCP8.5 scenarios, respectively. Wheat water demand was also projected to decrease by 13–42%, with peak demand occurring approximately two months earlier than at present. Koukouli et al. (2025) applied the CropSyst model together with field data (2016–2017) to examine the impact of climate change on maize yield and irrigation requirements in northern Greece Results demonstrated that under RCP4.5 and RCP8.5 scenarios for the future periods (2030–2050 and 2080–2100), changes in temperature and precipitation would alter the total irrigation needs with varying magnitudes.

Bakshi et al. (2022) investigated the effect of climate change on the yield of major cereals in Iran. Their findings demonstrated that the sensitivity of crops to precipitation and temperature is different across climatic zones; Specifically, in cold semi-arid climates, rainfed wheat exhibited the highest response to temperature, in warm semi-arid climates, rainfed barley, in temperate semi-arid climates, irrigated wheat, in cold dry climates, rainfed wheat, in warm dry climates, rainfed barley, and in temperate dry climates, rainfed wheat once again.

Afshartbar et al. (2023) analyzed the impacts of different climate scenarios on crop yield simulation, available water, cropping pattern shifts, and farmers' profitability in Marvdasht County. Climate projections for the region were generated using daily data and the LARS-WG downscaling method under RCP2.6, RCP4.5, and RCP8.5 scenarios for the period 2020–2080. Results indicated that the greatest yield reduction were observed for tomato, wheat, and rice crops, whereas yield increases were projected for alfalfa and barley**.** Soleimani Nejad et al. (2019) examined the effects of climate change on crop cultivation patterns in the Mashhad plain for the year 2031 using the GFA[2] function. Their results revealed that the most significant yield changes due to climatic conditions were associated with wheat and barley**.**

Considering the strategic role of Khorasan Razavi Province in wheat production, a comprehensive analysis of the impact of future climate scenarios on the yield and water productivity of irrigated wheat has not yet been conducted in this province. The present study employed a combination of the two models LARS-WG 8 and AquaCrop 7.1 to analyze climate scenarios for 2040 and to estimate wheat water productivity in Khorasan Razavi Province. The findings of this research can serve as a scientific foundation and practical reference for future planning in the field of agricultural water resources management and food security policymaking in Iran. In addition, the results of the study have been analyzed from a sustainability perspective, highlighting how climate change may influence the resilience of agricultural systems, the efficiency of resource utilization, and the assurance of long-term food security.

2. Materials and Methods

2.1. Study area

Khorasan Razavi Province is located in the northeast of Iran (fig. 1), covering an area of about 118,000 km^2, accounting for about 7% of the country's total area. The average annual rainfall ranges between 300 to 400 mm, but declines to nearly 150 mm in the southern, eastern, and central regions. Approximately 49.2% of the province is mountainous, while 50.8% is plains. Although the province exhibits diverse climatic conditions, it is generally classified as a semi-arid region of Iran (Aalijahan and Khosravichenar, 2021). According to Agricultural Yearbook (2023), this province, with about 171,000 hectares of irrigated wheat cultivation, ranks among the leading provinces in wheat production.

[2] Genetic Function Approximation

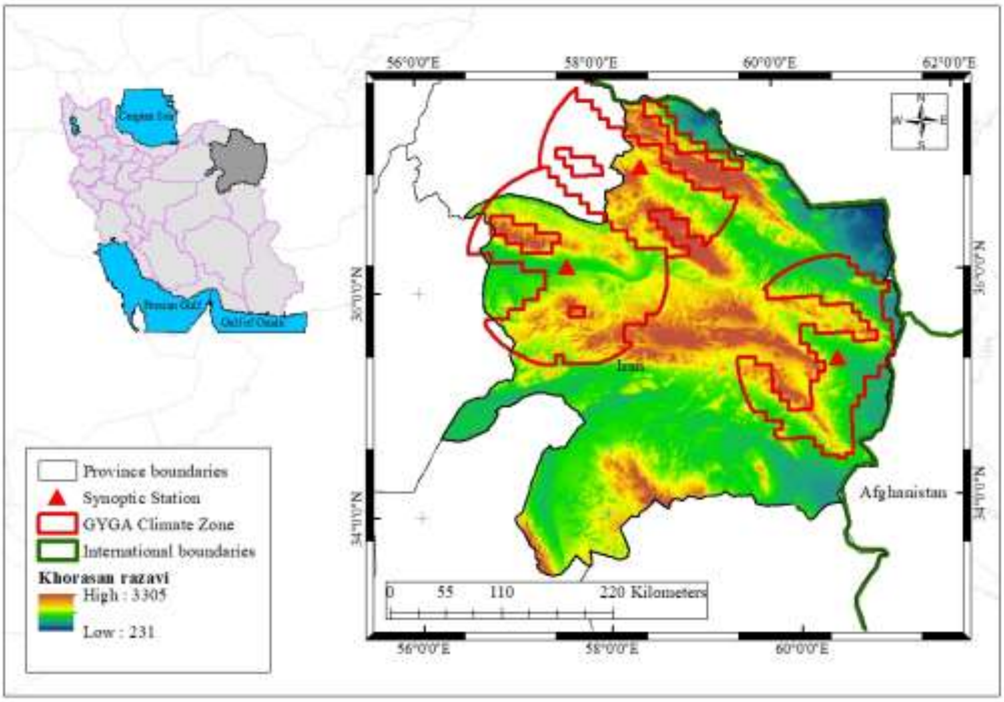

Figure 1. Geographical location of the study area

In this study, reference stations for wheat production were identified at the provincial level in accordance with the GIGA Protocol. The GYGA protocol is a globally recognized framework for analyzing and evaluating the potential for agricultural production, developed within the Global Yield Gap Atlas project. It integrates meteorological, climate data, and crop simulation models to provide accurate assessments of crop growth and production conditions at national and regional scales. By selecting reference meteorological stations and key climatic zones, the GIGA Protocol enables robust analysis at the national and regional scales and supports policymakers and researchers in identifying strategies to improve food security and agricultural sustainability (Soltani et al., 2019).

In the GYGA protocol, the country is initially divided into homogeneous climatic zones; these zones, known as District Climatic Zones (DCZs), which represent areas with similar conditions in terms of temperature, precipitation, and growing season length within a given area (Soltani et al., 2019). To determine the influence area of each meteorological station, a 100 km buffer is applied around it. By overlapping these buffers with climatic zoning maps, the precise boundaries of DCZs are delineated. Subsequently, meteorological stations that cover more than 1% of the national wheat cultivation area are designated as eligible reference stations (Van Bussel et al. 2015). Table 1 and Figure 1 show the characteristics and locations of the reference stations.

Table 1. Characteristics of meteorological reference stations

Station Name	Longitude (°)	Latitude (°)	Altitude (m)	Land area (ha)	Wheat area (%)	Areas covered
Quchan	58.5	37.07	1 287	26 491	1.2	Khushab, Takht-e Jolgeh, Nishapur, Quchan, Chenaran, Esfarayen, Shirvan, Farooj
Sabzvar	57.65	36.21	962	44 624	2	Kashmar, Bardaskan, Joghatai, Khushab, Nishapur, Takht-e Jolgeh, Sabzevar, Joveyn, Esfarayen
Torbat-e Jam	60.56	35.29	950	26 499	1.2	Bakharz, Zaveh, Khaf, Taybad, Roshtkhar, Torbat-e Jam

2.2. The AquaCrop model

AquaCrop is a crop simulation model developed by the Food and Agriculture Organization of the United Nations (FAO) and specifically designed to study the response of crops to different conditions (Steduto et al., 2007). Unlike many complex crop growth models, the model has a simplified yet scientifically robust structure**,** with its primary emphasis on water productivity and the relationship between evapotranspiration, canopy development and final yield (Sedhai et al. 2023). The model enables accurate evaluation of crop performance under different management and climatic conditions by simulating key processes such as vegetation growth, biomass accumulation, grain yield, and the impacts of water stress (Li et al. 2024). AquaCrop conceptualizes the soil, plant, atmosphere and management environments as an integrated system. Using climate and management inputs, the model first simulates the canopy cover to calculate transpiration as shown in Equation (1), then calculates biomass based on water productivity and actual evapotranspiration (Eq. 2), and finally estimates the economic yield (e.g., wheat grain yield) through allocation coefficients (Eq. 2) (Ahmadi et al. 2024). One of the major advantages of AquaCrop is that the number of plant parameters is limited and can be calibrated, making it particularly suitable for regions with restricted data availability**.**

$$T_r = Ks\ Ks_{TR}\ CC^*\ Kc_{Tr,X}\ ET_0 \qquad (1)$$

$$B = WP^* \sum {}^{Tr}/_{ET_0} \qquad (2)$$

$$Y = f_{HI} HI_0\ B \qquad (3)$$

ET_0: Potential evapotranspiration
$Kc_{Tr,X}$: Relative crop transpiration coefficient
CC^*: Adjusted canopy cover to eliminate inter-row air flow effects
Ks_{Tr}: Temperature stress coefficient
Ks: Stomatal closure coefficient (water stress, between 0 and 1)
WP^*: Normalized water productivity
HI_0: Reference harvest index (HI at physiological maturity)
f_{HI}: Adjustment factor for the effect of stresses on harvest index

The inputs to the AquaCrop model are organized into four major categories**,** each representing a part of the soil-plant- atmosphere system. Climatic inputs include precipitation, minimum and maximum temperatures, reference evapotranspiration, and CO_2 concentration, which determine the environmental conditions for crop growth (Steduto et al. 2007). Soil inputs encompass soil type and texture, water holding capacity (FC and PWP), hydraulic conductivity, soil depth and stratification (Steduto et al. 2009). In the plant section, parameters such as crop type, phenological stages, crop expansion rate, water productivity and root development are entered to simulate physiological characteristics and crop response to environmental conditions (Dehghani et al. 2019). Finally, management inputs include planting date, irrigation scheduling and method, fertilization practices, and plant density (Raes et al. 2009).

In recent versions of the AquaCrop model, the capability to simulate the effect of increasing atmospheric CO_2 concentrations and to incorporate output of large-scale climate models (GCM/RCM) based on RCP or SSP scenarios has been introduced. These enhancements allow the model to more accurately represent the impacts of future climate change. (FAO, 2018). In this study, meteorological data for the period 1995–2024 were obtained from the National Meteorological Organization and used to prepare the meteorological input files. Reference evapotranspiration during this period was calculated using the standard FAO Penman–Monteith method.

Climate data from the year 2040 were generated using the LARS WG model, and given that only minimum and maximum temperature values were available in the model output, reference evapotranspiration for 2040 was estimated using the Hargreaves–Samani method. Furthermor, the remaining model input parameters were calibrated based on the information reported by Zeinali Mobarakeh et al. (2018, 2019) so that phenological parameters and plant characteristics were most aligned with the actual conditions of the region. The weighted average of wheat yield was calculated for Khorasan Razavi Province based on the cultivated area within each buffer. Table 2 presents the calibrated coefficients in the model, which were adjusted to reflect local conditions and ensure accurate simulation of crop growth and yield.

.

Table 2. Plant characteristics used in the model calibration phase

Factor	Symbol	Unit	Value
Base temperature for growth	T_{base}	°C	1
Upper temperature threshold	T_{upper}	°C	30
Maximum rooting depth	zr_{min}	m	1.50
Minimum rooting depth	zr_{max}	m	0.30
Initial canopy cover at 90% emergence	CC_0	%	6.45
Canopy growth coefficient	CGC	°/day	4.10
Canopy decline coefficient	CDC	°/day	9.4
Maximum canopy cover	CC_{max}	%	96
Reference harvest index	HI_0	%	45
Upper threshold of soil moisture depletion for canopy expansion	P_{upper}	-	0.20
Lower threshold of soil moisture depletion for canopy expansion	P_{lower}	-	0.65
Upper threshold of soil water stress coefficient for canopy senescence	P_{upper}	-	0.70
Normalized water productivity	WP^*	gr/m^2	15.10
Crop transpiration coefficient	$Kc_{Tr,X}$	-	1.10
Shape factor of soil water stress coefficient for canopy expansion	Shape factor	-	2
Upper threshold of soil moisture depletion for stomatal control	P_{upper}	-	0.65
Shape factor of soil water stress coefficient for stomatal control	Shape factor	-	2.5
Shape factor of soil water stress curve for canopy senescence	Shape factor	-	2.5
Flowering duration		day	12
Time from sowing to emergence	-	day	8
Time from sowing to flowering	-	day	141
Time from sowing to max canopy	-	day	137
Time from sowing to maturity	-	day	195

2.3. LARS-WG model

The LARS-WG 8 model was used to generate climate data for the horizon 2040 (serving as climate data input for the AquaCrop model) (Ahmadi et al. 2024). LARS-WG model is one of the most widely used stochastic weather generators for producing daily climate data at the local scale (Dehghani et al. 2026). This model is particularly valuable when short-term observational records are incomplete or insufficient and the researcher needs to produce long-term time series consistent with the regional climate (Semenov and Stratonovitch, 2010). Using advanced statistical techniques, LARS-WG extracts the climatic characteristics of a station from historical observations and generates synthetic yet realistic datasets of precipitation, temperature and solar radiation that are statistically consistent with actual climate conditions (Lotfi et al. 2022). The core of the model relies on probability distributions and wet–dry day transition patterns**.** Precipitation is simulated by estimating the probability of rainy and dry days and the distribution of rainfall amounts on wet days. For minimum and maximum temperatures and solar radiation, appropriate statistical distributions are applied to accurately capture daily and seasonal variability (Obead and Hussein, 2024; Semenov and Stratonovitch, 2010).

One of the key strengths of LARS-WG is its ability to account for interdependence among climatic variables (e.g.,the relationship between precipitation and temperature) and produce data that is physically plausible. Beyond producing synthetic climate data, LARS-WG is an essential tool in climate change research (Ahmadi et al. 2024). This model can incorporate outputs from general circulation models (GCM) for different

IPCC[3] scenarios and downscale future climate projections to the local scale (Lotfi et al. 2022). In this way, the influence of RCP or SSP scenarios on precipitation and temperature at the station level can be assessed. This capability has led to the widespread application of LARS-WG in agricultural research, water resources, drought management and climate change impact assessment (Obead and Hussein, 2024; Ahmadi et al. 2024).

In the downscaling process with the LARS-WG model, the outputs of different global climate models (GCM) are typically employed to address the uncertainties arising from the model structure. However, studies conducted in Iran have demonstrated that some models perform more effectively in reproducing the country's temperature and precipitation patterns. Among the models applied, HadGEM3-GC31-LL has exhibited stronger agreement with observational records across many regions of Iran; for this reason, it has been adopted in recent studies as one of the reliable options for climate downscaling in Iran (Dastorani et al. 2025; Bagheri Khaneghahi et al. 2025; Ahmadi et al. 2024; Dehghani et al. 2026). In this study, the model was calibrated using data from 1995 to 2024, and subsequently employed to generate climate projections for the year 2040 under three scenarios: SSP1-2.6, SSP2-4.5, and SSP5-8.5. Figure 2 illustrates the trend in CO_2 concentration and its variation across different climate scenarios (IPCC, 2021).

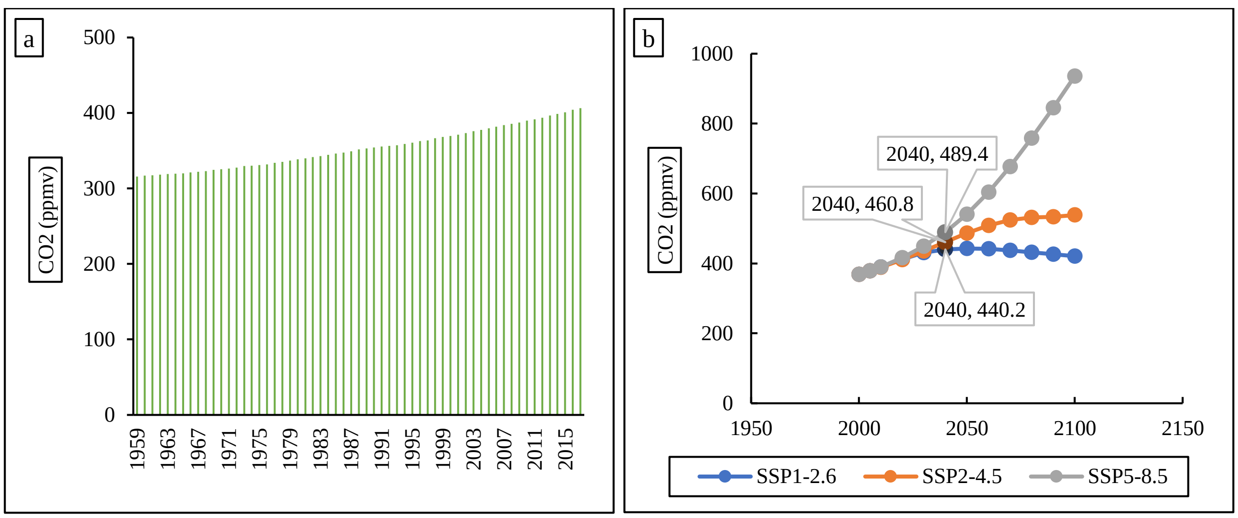

Figure 2. Historical Trend of Atmospheric CO_2 Concentration (a); Atmospheric CO_2 Concentration under Different Climate Scenarios (b)

Figure 3 illustrates the trends in precipitation as well as minimum and maximum temperatures over the last 30 years (1995–2024) for three reference meteorological stations, based on data obtained from the Iran Meteorological Organization (IRIMO).

[3] Intergovernmental Panel on Climate Change

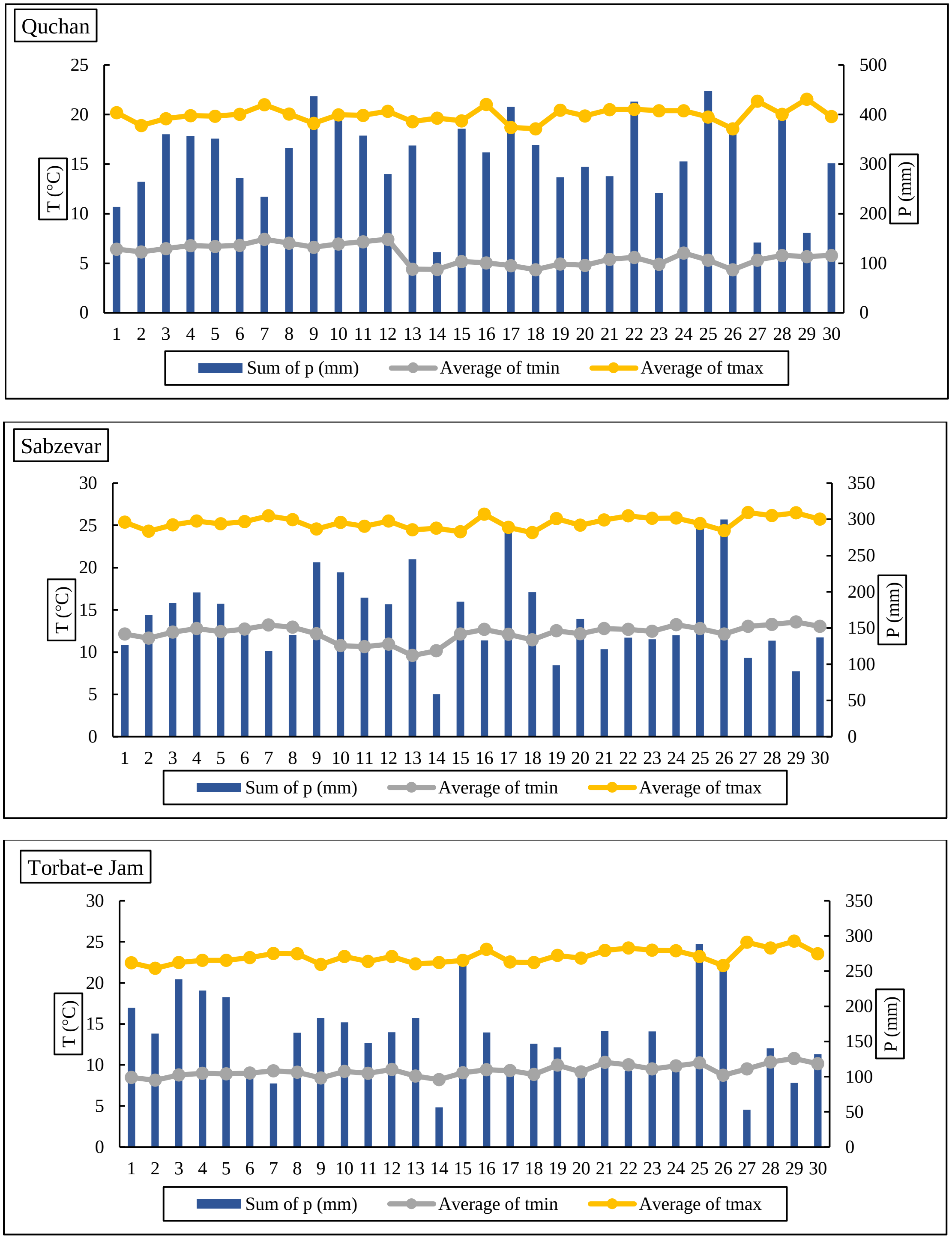

Figure 3. Trends in Precipitation and Temperature Variables Over the Past 30 Years at Three Reference Stations (1995-2024)

2.4. Mann–Kendall Trend Analysis

The Mann–Kendall test is a non-parametric method used to identify monotonic trends in time-series data, characterized by low sensitivity to outliers and abrupt shifts. Without requiring assumptions of normality or randomness, this test evaluates whether an increasing or decreasing trend exists over time (Raoufi and Attayee, 2025).

In the Mann–Kendall test, the statistics S and Z work together to determine both the direction and the significance of a trend in a time series. The statistic S is calculated by comparing all possible data pairs and indicates whether increasing or decreasing changes dominate the series; therefore, a positive S reflects an increasing trend, a negative S indicates a decreasing trend. To evaluate the statistical significance of this trend, S is standardized using its variance to obtain the Z statistic. The sign of Z confirms the direction of the trend, while the absolute value of Z reflects the confidence level associated with the detected trend. Common significance thresholds include $|Z| > 1.96$ (95% confidence) (Ahmadpari et al., 2025). In this study, the significance of trends was assessed using the Mann–Kendall test implemented in the PAST software.

2.5. LARS-WG performance metrics

To assess the accuracy of the LARS-WG model in simulating climate variables, a set of statistical indices including the mean, the standard deviation, T-test, and F-test was used. These indices allow for direct comparison between observational data and data generated by the model and indicate the model's ability to reproduce average values and monthly fluctuations (Table 3).

Table 3. Statistical Indices for LARS-WG Model Performance Evaluation (Ledolter et al., 2020)

Index	Scientific Definition	Formula
Mean obs (Observed Mean)	Mean of observed data during the baseline period	$Mean_{obs} = \frac{1}{n} \times \sum_{i=1}^{n} X_{obs,i}$
Mean gen (Generated Mean)	Mean of the model-generated data	$Mean_{gen} = \frac{1}{n} \times \sum_{i=1}^{n} X_{gen,i}$
SD obs (Observed Standard Deviation)	Variability (standard deviation) of the observed data	$SD_{obs} = \sqrt{\left(\frac{1}{n-1}\right) \times \Sigma\left(X_{obs,i} - Mean_{obs}\right)^2}$
SD gen (Generated Standard Deviation)	Variability (standard deviation) of the generated data	$SD_{gen} = \sqrt{\left(\frac{1}{n-1}\right) \times \Sigma\left(X_{gen,i} - Mean_{gen}\right)^2}$
T-Statistic	Test for the difference between observed and generated means	$t = \frac{Mean_{obs} - Mean_{gen}}{\sqrt{(SD_{obs}{}^2 / n_{obs}) + (SD_{gen}{}^2 / n_{gen})}}$
T-Test p-value	Probability of observing the mean difference (p-value)	—
F-Statistic	Test for comparing the variances of observed and generated data	$F = \frac{SD_{obs}{}^2}{SD_{gen}{}^2}$
F-Test p-value	Probability of observing the variance difference (p-value)	—

$X_{obs,i}$: Observed value of the climatic variable at time i
$X_{gen,i}$: Simulated value of the climatic variable by the LARS-WG model at time i
n: Total number of data points (number of days, months, or years depending on the analysis)
$Mean_{obs}$ (or $\bar{X}_{obs}$): Mean of the observed data
$Mean_{gen}$ (or $\bar{X}_{gen}$): Mean of the generated (simulated) data
SD_{obs}: Standard deviation of the observed data
SD_{gen}: Standard deviation of the generated (simulated) data
n_{obs}: Number of observed data points
n_{gen}: Number of generated data points
t: Value of the t-test statistic used to compare the means
F: Value of the F-test statistic used to compare the variances

p-value: Probability of statistical significance for the difference in means or variances in the t-test and F-test

In evaluating model performance, the closeness of simulated means to observed means indicates the model's ability to reproduce the central value of the variable. Comparison of standard deviations indicates the extent to which the model is able to represent data fluctuations and dispersion (Wilks, 2011). The T-test is used to measure the significance of the difference in means; where p values greater than 0.05 indicate no significant difference and therefore an appropriate simulation of the mean (Student, 1908). The F-test is also used to compare variances, and p values greater than 0.05 indicate that the model has reproduced fluctuations correctly, while values less than 0.05 indicate a significant difference and a weakness in simulating data dispersion (Fisher, 1970).

2.6. AquaCrop Model performance metrics

In this study, to evaluate the quality of AquaCrop model outputs in predicting grain yield, a set of the following statistical indices was employed.

$$\mathrm{NRMSE} = \frac{1}{\mathrm{O}}\sqrt{\frac{\sum_{i=1}^{n}(\bar{\mathrm{O}}_{i} - \mathrm{P_i})^2}{n}} \quad (4)$$

$$\mathrm{NSE} = 1 - \frac{\sum_{i=1}^{n}(O_{i} - \mathrm{P_i})^2}{\sum_{i=1}^{n}(O_{i} - \bar{\mathrm{O}}_i)^2} \quad (5)$$

$$\mathrm{CRM} = \frac{\sum_{i=1}^{n}\mathrm{O_i} - \sum_{i=1}^{n}\mathrm{P_i}}{\sum_{i=1}^{n}\mathrm{O}} \quad (6)$$

$$\mathrm{d} = 1 - \frac{\sum_{i=1}^{n}(\mathrm{P}_{i} - \mathrm{O_i})^2}{\sum_{i=1}^{n}(|\mathrm{P_i} - \bar{\mathrm{O}}_i| + |\mathrm{O_i} - \bar{\mathrm{O}}_i|)^2} \quad (7)$$

In the presented equations, O_i، P_i ،$\bar{\mathrm{O}}_i$ and n represent the measured values, simulated values, the mean of the measured values, and the total number of observations, respectively. The NRMSE (Normalized Root Mean Square Error) index is used as a criterion for evaluating the accuracy of the simulation model; lower values, approaching zero, indicate a higher agreement between the simulated results and the experimental data (Dehghani et al, 2026). The CRM (Coefficient of Residual Mass) reflects the relative difference between simulated and measured values. Positive CRM values indicate that the model, on average, underestimates the actual values, whereas negative CRM values show that the model tends to overestimate them (Chauhdary et al., 2024). Moreover, values close to one for NSE (Nash–Sutcliffe efficiency) and d (index of agreement) demonstrate a strong consistency between simulated and measured data, confirming the reliability of the model (Ahmadpari et al., 2020).

3. Results and Discussion

3.1. Significance of Climatic Trends

The results from the three stations show that precipitation exhibits no statistically significant trend in Quchan, Sabzevar, or Torbat-e Jam, as the Z values remain below the 1.96 threshold. In contrast, minimum and maximum temperatures display clearer warming signals: Tmin shows a significant increasing trend in Sabzevar and Torbat-e Jam, and Tmax also increases significantly in Torbat-e Jam. These findings indicate that climatic warming in the region is primarily reflected through rising minimum and maximum temperatures, while precipitation remains highly variable and trend-free. Such patterns have important implications for water resources, evapotranspiration rates, and agricultural water requirements (Nhemachena et al., 2020).

Table 4. Mann–Kendall Test Results

Station Name	Parameter	S	Z	Trend Detection	Significance
Quchan	P	7	0.11	Increasing	NO
	Tmin	-104	1.84	Decreasing	NO
	Tmax	62	1.09	Increasing	NO
Sabzevar	P	-53	0.92	Decreasing	NO
	Tmin	134	**2.38**	Increasing	YES
	Tmax	104	1.84	Increasing	NO
Torbat-e Jam	P	-107	1.89	Decreasing	NO
	Tmin	234	**4.16**	Increasing	YES
	Tmax	181	**3.21**	Increasing	YES

and observed mean data are not significantly different. However, the F-test p-values are almost 0.0 for Tmin and Tmax in all months, indicating that the model systematically underestimates the monthly temperature dispersion and fluctuations. The situation is more favorable for precipitation, with only a few months (such as March and April in Quchan and Sabzevar) showing significant differences in variance.

3.2. Evaluation of the LARS WG

Tables 5 to 7 reveal a clear and consistent pattern at all three stations of Quchan, Sabzevar and Torbat-e Jam. The LARS WG model performs very well in simulating the monthly mean precipitation, Tmin and Tmax, as the Student's t-test p-values **exceed** 0.05 in most months, indicating that the simulated

Table 5. Statistical performance indicators of the LARS-WG model for precipitation, Tmin, and Tmax at Quchan station

P	Jan	Feb	Mar	Apr	May	Jun	Jul	Aug	Sep	Oct	Nov	Dec
T-student statistic	-0.1	1.1	-0.4	-0.2	-1.8	-1.2	0.2	-0.3	-1.0	-0.1	-0.1	-0.7
T-student p-value	0.9	0.3	0.7	0.8	0.1	0.2	0.9	0.8	0.3	1.0	0.9	0.5
F statistic	1.3	1.3	1.0	2.1	1.2	1.3	1.1	1.9	2.2	1.2	1.1	1.7
F p-value	0.4	0.4	1.0	0.0	0.7	0.4	0.9	0.1	0.0	0.6	0.8	0.1
T_{min}	Jan	Feb	Mar	Apr	May	Jun	Jul	Aug	Sep	Oct	Nov	Dec
T-student statistic	0.4	0.3	0.4	0.3	0.0	1.2	0.3	-0.5	-0.6	0.5	-0.3	-0.9
T-student p-value	0.7	0.8	0.7	0.8	1.0	0.2	0.8	0.6	0.6	0.6	0.8	0.4
F statistic	10.6	11.9	3.9	4.1	5.5	4.6	7.2	12.4	9.3	11.5	7.3	10.4
F p-value	0.0	0.0	0.0	0.0	0.0	0.0	0.0	0.0	0.0	0.0	0.0	0.0
T_{max}	Jan	Feb	Mar	Apr	May	Jun	Jul	Aug	Sep	Oct	Nov	Dec
T-student statistic	0.5	-0.6	-1.0	0.1	1.2	1.8	0.0	1.9	0.6	0.3	-0.3	-0.4
T-student p-value	0.6	0.6	0.3	0.9	0.2	0.1	1.0	0.1	0.6	0.8	0.8	0.7
F statistic	10.1	8.9	5.1	5.1	5.6	4.2	5.5	6.2	2.7	4.6	5.6	8.1
F p-value	0.0	0.0	0.0	0.0	0.0	0.0	0.0	0.0	0.0	0.0	0.0	0.0

Table 6. Statistical performance indicators of the LARS-WG model for precipitation, Tmin, and Tmax at Sabzevar station

P	Jan	Feb	Mar	Apr	May	Jun	Jul	Aug	Sep	Oct	Nov	Dec
T-student statistic	-0.5	-0.3	1.0	-0.5	-0.1	-0.6	0.6	-0.9	0.2	-1.0	0.5	-0.5
T-student p-value	0.6	0.7	0.3	0.6	0.9	0.5	0.6	0.4	0.8	0.3	0.6	0.6
F statistic	1.4	1.1	2.0	2.2	1.1	1.4	1.5	1.3	1.9	1.8	1.5	1.1
F p-value	0.3	0.7	0.0	0.0	0.8	0.4	0.2	0.5	0.1	0.1	0.2	0.8
T_{min}	Jan	Feb	Mar	Apr	May	Jun	Jul	Aug	Sep	Oct	Nov	Dec
T-student statistic	0.5	0.3	-0.6	-0.5	0.4	1.2	1.0	1.8	0.2	1.4	-0.5	-0.4
T-student p-value	0.7	0.8	0.6	0.7	0.7	0.2	0.3	0.1	0.8	0.2	0.7	0.7
F statistic	13.6	5.7	4.5	5.4	6.1	6.9	8.6	11.0	10.4	7.1	7.1	7.3
F p-value	0.0	0.0	0.0	0.0	0.0	0.0	0.0	0.0	0.0	0.0	0.0	0.0
T_{max}	Jan	Feb	Mar	Apr	May	Jun	Jul	Aug	Sep	Oct	Nov	Dec
T-student statistic	0.9	0.1	-0.8	0.3	-0.5	1.2	0.7	1.8	0.9	1.5	-0.2	0.0
T-student p-value	0.4	0.9	0.4	0.8	0.7	0.2	0.5	0.1	0.4	0.1	0.8	1.0

P	Jan	Feb	Mar	Apr	May	Jun	Jul	Aug	Sep	Oct	Nov	Dec
F statistic	9.4	6.7	5.4	7.3	7.2	7.9	5.5	3.2	4.6	4.6	5.9	15.5
F p-value	0.0	0.0	0.0	0.0	0.0	0.0	0.0	0.0	0.0	0.0	0.0	0.0

Table 7. Statistical performance indicators of the LARS-WG model for precipitation, Tmin, and Tmax at Torbat-e Jam station

P	Jan	Feb	Mar	Apr	May	Jun	Jul	Aug	Sep	Oct	Nov	Dec
T-student statistic	-0.8	0.7	-0.8	1.2	0.9	-0.6	0.4	-0.2	-1.6	0.4	-0.8	-0.2
T-student p-value	0.4	0.5	0.4	0.2	0.4	0.6	0.7	0.9	0.1	0.7	0.4	0.8
F statistic	1.1	1.5	1.4	2.0	1.2	2.5	2.4	1.2	6.4	1.1	1.5	1.4
F p-value	0.8	0.2	0.3	0.0	0.6	0.0	0.0	0.5	0.0	0.8	0.3	0.4
T_{min}	Jan	Feb	Mar	Apr	May	Jun	Jul	Aug	Sep	Oct	Nov	Dec
T-student statistic	0.5	0.2	0.1	0.2	-0.1	1.1	1.0	3.2	0.1	-0.5	-0.3	-0.6
T-student p-value	0.6	0.9	0.9	0.8	1.0	0.3	0.3	0.0	0.9	0.6	0.8	0.6
F statistic	14.4	5.7	4.0	2.9	12.1	5.2	2.8	2.5	3.6	8.6	4.6	4.0
F p-value	0.0	0.0	0.0	0.0	0.0	0.0	0.0	0.0	0.0	0.0	0.0	0.0
T_{max}	Jan	Feb	Mar	Apr	May	Jun	Jul	Aug	Sep	Oct	Nov	Dec
T-student statistic	1.2	-0.1	-0.9	-0.8	0.0	2.3	-0.5	2.4	0.2	0.7	-0.7	0.4
T-student p-value	0.3	0.9	0.4	0.4	1.0	0.0	0.7	0.0	0.8	0.5	0.5	0.7
F statistic	13.9	6.9	4.7	5.3	4.1	5.3	6.0	2.3	4.5	4.9	4.7	6.1
F p-value	0.0	0.0	0.0	0.0	0.0	0.0	0.0	0.0	0.0	0.0	0.0	0.0

Previous studies have also shown that the LARS WG model performs reasonably well in simulating mean precipitation and temperature (Hadi et al., 2024; Komasi and Doorbashizadeh, 2025; Dehghani et al., 2026), but it is usually limited in capturing temperature dispersion and fluctuations (Semenov and Brooks., 1999; Ababaei et al., 2010; Khalili et al., 2016; Calanca, 2020). For example, in the study of Khalili et al. 2016, the results of model validation showed that mean precipitation and temperature did not differ significantly from observational data, but the model tended to underestimate the standard deviation of temperature. The results of Kavwenje et al. (2022) showed that the LARS WG model simulates temperature with much higher accuracy than precipitation. In contrast, precipitation forecasts are associated with high uncertainty. The LARS WG model performs much better in simulating temperature than precipitation and under-represents temperature variability (Calanca, 2020). Overall, the results indicate that the model is very accurate in reproducing the climate mean, it systematically underestimates monthly variability**,** particularly for temperature, a pattern consistently observed at all three stations (Figure 4).

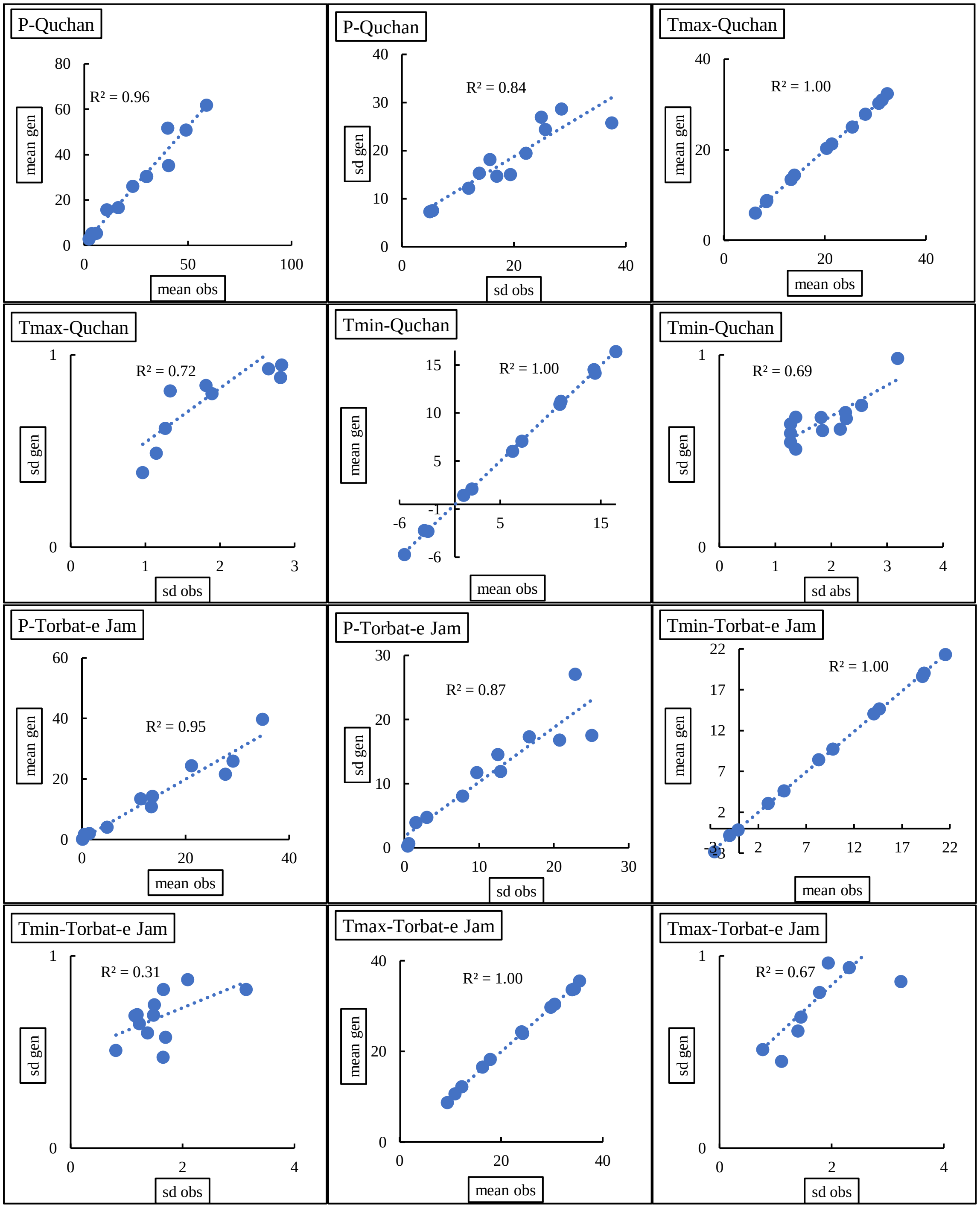
P-Quchan
R² = 0.96
mean gen
mean obs
P-Quchan
R² = 0.84
sd gen
sd obs
Tmax-Quchan
R² = 1.00
mean gen
mean obs
Tmax-Quchan
R² = 0.72
sd gen
sd obs
Tmin-Quchan
R² = 1.00
mean gen
mean obs
Tmin-Quchan
R² = 0.69
sd gen
sd abs
P-Torbat-e Jam
R² = 0.95
mean gen
mean obs
P-Torbat-e Jam
R² = 0.87
sd gen
sd obs
Tmin-Torbat-e Jam
R² = 1.00
mean gen
mean obs
Tmin-Torbat-e Jam
R² = 0.31
sd gen
sd obs
Tmax-Torbat-e Jam
R² = 1.00
mean gen
mean obs
Tmax-Torbat-e Jam
R² = 0.67
sd gen
sd obs

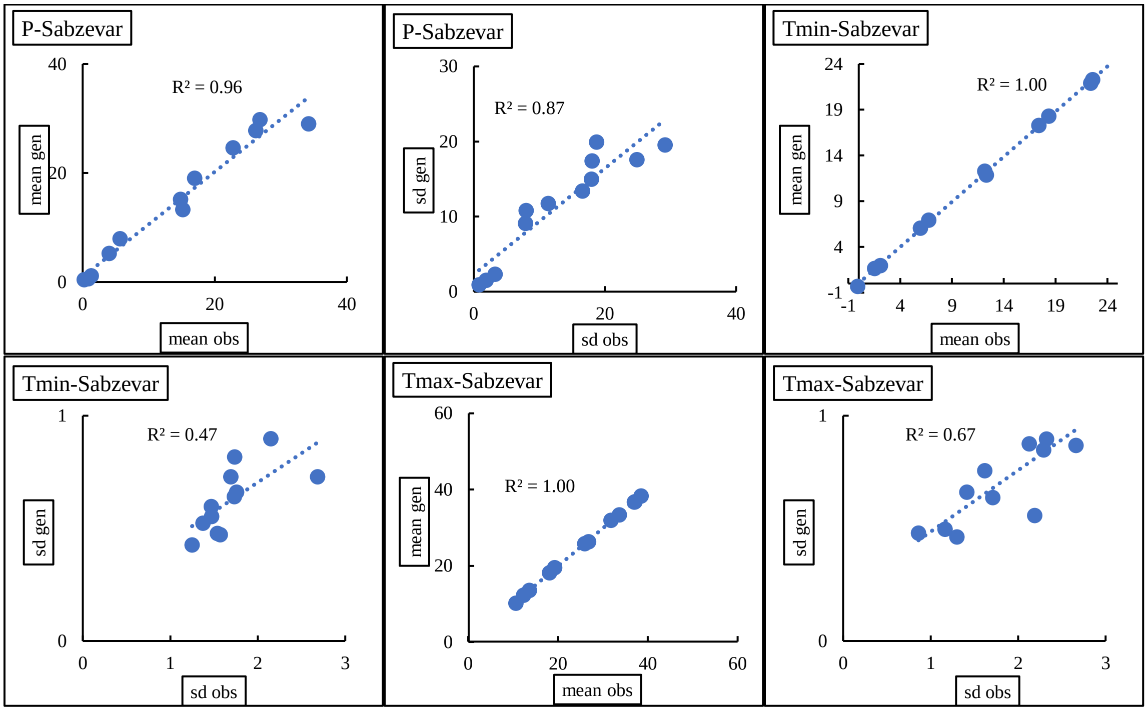

Figure 4. Monthly mean and standard deviation for minimum and maximum temperature and precipitation

3.3. Climate change in 2040

The patterns presented in Figure 5 show that annual mean temperature in all three stations, Quchan, Sabzevar, and Torbat-e Jam has an increasing trend in the future (2040) under different emission scenarios. A baseline comparison of 2010–2024 with future scenarios shows that this increase is relatively limited in the low-emission scenario SSP1-2.6, but becomes more pronounced in the intermediate scenario and especially the high-emission scenario SSP5-8.5. The highest temperature is observed in Quchan, where the mean temperature rises from 12.7°C to 14.1°C in the SSP5-8.5 scenario.

Zenozi Alamdari et al. (2025) showed that in all scenarios, annual temperature will increase by 0.3 to 2.8°C in all regions of Khorasan Razavi Province by 2100. The results of the study by Usta et al. (2022), using 22 CMIP6 models showed that Iran will reach the warming thresholds of 1.5, 2.0 and 2.5°C faster than the global average. The trends show that warming in Iran is more severe than the global mean. Recent studies, such as Naderi et al. (2025), have shown that under the SSP5-8.5 emission scenario, Iran will face a significant increase in temperature in all seasons, especially in summer when the greatest intensity of warming occurs. Zynal Zadeh et al. (2025) demonstrated, by studying the Torbat-Heydariyeh and Kashmar stations, that under the SSP2-4.5 and SSP5-8.5 scenarios, extreme climate indices such as minimum and maximum temperatures and heavy precipitation will increase between 2026 and 2100.

While the present analysis focuses primarily on changes in mean climatic variables, it is important to note that extreme events, such as heatwaves, drought episodes, and intense precipitation, play a decisive role in wheat growth and yield stability. Recent studies in Iran have shown that under high-emission scenarios, the frequency and intensity of extreme temperature indices, including very high maximum temperatures and warm nights, are projected to increase substantially (Najafi et al., 2024). Such extremes can induce heat stress during sensitive phenological stages, accelerate crop development, reduce grain filling duration, and intensify water deficits even when mean temperature changes appear moderate.

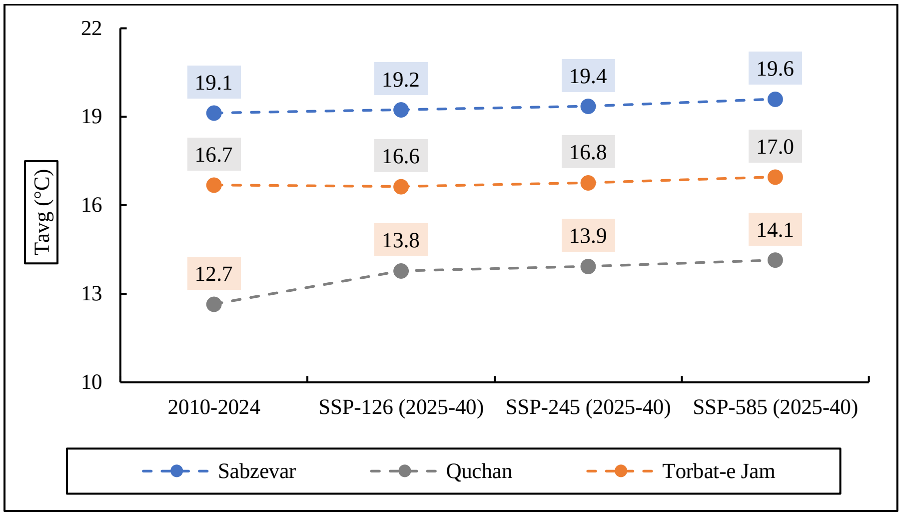

Figure 5. Changes in average temperature

According to Figure 6, the results indicate that under future climate scenarios, precipitation will increase by 11 to 38%, while reference evapotranspiration is expected to decrease by 8–32%. It should be noted that spatial and seasonal heterogeneity of precipitation is highly important. Some models show increases in winter and decreases in summer (Usta et al., 2022; Naderi et al., 2025), which convey different implications for water resource management and agriculture. The reduction in reference evapotranspiration in future scenarios is primarily associated with a decrease in the amplitude of daily temperature fluctuations. The results indicate that the minimum temperature increases by up to 2.2°C, while the maximum temperature changes range from -0.8 to +1°C. This convergence between minimum and maximum temperatures reduces the slope of the daily thermal gradient and, consequently leads to a decline in reference evapotranspiration.

The projected decrease in reference evapotranspiration (ET_0) under future climate scenarios, despite increasing air temperature, is primarily attributed to a substantial reduction in the diurnal temperature range (DTR). In the studied region, minimum temperature exhibits a stronger increase compared to maximum temperature, resulting in a pronounced narrowing of DTR. Because the Hargreaves–Samani equation is highly sensitive to the $(Tmax-Tmin)^{0.5}$ term, the reduction in DTR exerts a dominant influence on ET_0 and outweighs the effect of the moderate increase in mean temperature. From a physical standpoint, a declining DTR is a well-established indicator of climate change and is often associated with increased nighttime cloudiness, higher atmospheric humidity, and reduced net radiative cooling. These conditions suppress the atmospheric evaporative demand, thereby lowering ET_0 even under overall warming. Similar findings have been reported in previous studies, confirming that changes in the structure of the daily temperature cycle can significantly modify evaporative demand and lead to reduced ET_0 under warming climates (Wang and Stjern, 2020; Stjern et al., 2020). This reduction can alter evapotranspiration patterns and plant water requirements (Üneş et al., 2020; Shakoor et al., 2020).

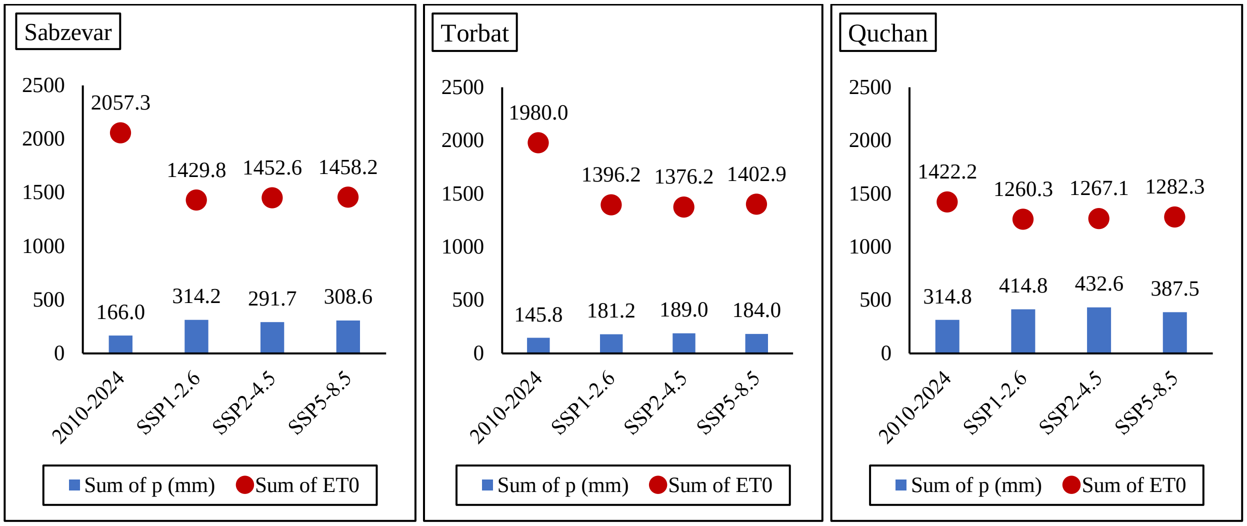

Figure 6. Changes in precipitation and reference evapotranspiration

3.4. AquaCrop Model Performance

The results indicate that the model has performed very well. An NSE of 0.92 shows that 92% of the variability in the observed data is explained by the model, which is considered “very good”. An NRMSE of 4% (RMSE = 0.26 t ha^{-1}) reflects very low error and high predictive accuracy. The CRM value of +0.04 suggests that the model has a very slight tendency toward overestimation, but this bias is minimal and does not meaningfully affect the overall model quality. Additionally, d = 0.99 indicates an almost perfect agreement between the simulated and observed data. Similar findings were also reported by Abedinpour (2021) and da Conceição et al. (2024), who confirmed the accuracy of the AquaCrop model.

Abedinpour (2021) showed that the AquaCrop model, with an error range of RMSE = 0.24–0.36 t ha^{-1}, NRMSE = 6–7.2%, and model performance values of E = 0.87–0.90 and d = 0.90–0.93, is capable of accurately simulating wheat yield under conditions of water stress and varying nitrogen supply. da Conceição et al. (2024) reported that the AquaCrop model showed acceptable accuracy in simulating bean yield, with a high R^2, an RMSE on the order of several hundred kilograms per hectare, an NRMSE below 15%, and a Willmott agreement index (d) ranging from 0.80 to 0.90.

3.5. Wheat yield and water productivity analysis in 2040

The results indicate that wheat yield increases across all three stations under every climate scenario by 2040 (Table 8), with the greatest enhancement occurring under the SSP5-8.5 scenario. Various studies in Iran and around the world have shown that wheat yield will increase in some regions under future climate scenarios, especially under SSP5-8.5, during the first half of the century (Mirshekari et al., 2025; Ahmadi et al., 2024; Ye et al., 2020). For example, research in the arid regions of southeastern Iran has shown that wheat yield will increase significantly by 2050 under SSP2-4.5 and SSP5-8.5, mainly due to the effect of high CO_2 concentration and improved water use efficiency (Mirshekari et al., 2025).

In colder regions such as East Azerbaijan, an increase in yield of up to 16% has also been reported**,** which is attributed to a longer growing season and more suitable temperature conditions for photosynthesis (Nazari et al., 2021). Global IPCC AR6 data also confirm that at higher latitudes, wheat yields will increase under SSP5-8.5 in the first half of the century, although the negative effects of warming will dominate by the end of the century (IPCC, 2021b). Simulation studies in China and Central Asia also show that wheat yields will increase under SSP5-8.5 in the 2020–2050 period, especially in semi-arid regions, mainly due to improved photosynthesis under high CO_2 conditions and a shift in the timing of plant growth (Ye et al., 2020).

Table 8. Changes in wheat yield in 2040 under different climate scenarios

Station Name	2010	2024	2040-SSP1-2.6	2039-40-SSP2-4.5	2039-40-SSP5-8.5
Sabzevar	6140	7257	7914	7990	8402
Quchan	7283	7679	8114	8269	8408
Torbat-e Jam	5438	6947	7314	7346	7695

The average wheat yield has increased from 6259.6 kg in 2010 to 7287.4 kg in 2024 and is projected to reach 8211.7 kg under the SSP5-8.5 scenario, reflecting a sustained upward trend in yield**.** At the same time, water productivity (WP) has improved by about 13% compared to 2024 (Figure 7). According to the results of Soltani et al. (2019), water productivity in Khorasan province is estimated to be 1.7 kg/m^3 on average.

The results of this study also show that under conditions of full irrigation and appropriate agricultural management water productivity increases to 2.09 kg/m^3 by 2050 under the RCP 8.5. Moreover, Zeinali Mobarakeh et al. (2018) reported reported that wheat yield in 2050 would increase by 1 to 13% under the RCP emission scenarios.

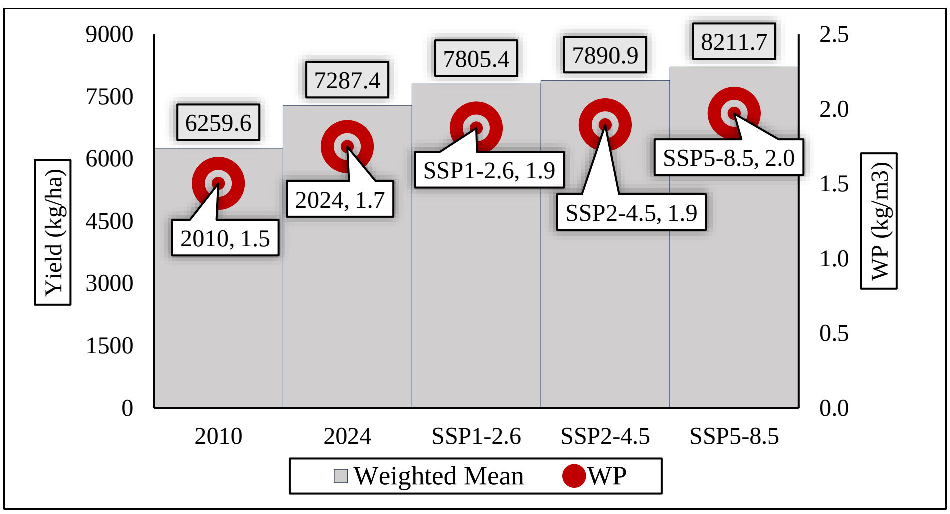

Figure 7. Changes in wheat yield and water productivity under different climate scenarios in Khorasan Razavi Province

3.5. Sustainability Perspective

Increasing wheat yields in future scenarios, even with an upward trend in average yield, does not necessarily indicate long-term sustainability of production. It has been repeatedly emphasized in the scientific literature that yield growth in climate scenarios can be short-lived or highly dependent on specific modeling assumptions**,** and in practice may be influenced by a set of negative factors resulting from climate change (Xu et al., 2024; Zare et al., 2025). while increasing temperature and carbon dioxide concentrations may accelerate plant growth and increase yield in the short term over the long-term, they can shorten the life cycles of pests and diseases and increase their number of generations. Studies show that many key wheat pests, such as aphids and wheat thrips, produce additional generations and exhibit greater damage severity at higher temperatures (Skendžić et al., 2021). The findings suggest that climate change could reduce the effectiveness of natural enemies of pests and increase the risk of future pest outbreaks (Wang et al., 2024). This could offset part of the yield advantage projected in future scenarios or even lead to yield reductions**.**

On the other hand, increasing temperatures and changing precipitation patterns can exacerbate physiological stresses such as heat stress during the flowering stage, reduced grain filling, and increased evaporation from the soil surface (Mirosavljević et al., 2024; Qi et al., 2022). Even if precipitation increases in some scenarios, its temporal distribution may become more irregular, with heavy and short-term rainfall events occurring instead of more uniform rainfall, thereby reducing water use efficiency (Suo et al., 2025). This issue has been highlighted in IPCC reports as one of the main challenges for agriculture in arid and semi-arid regions. Another important factor is the decline in soil quality due to increasing temperatures, enhanced erosion, and a decrease in organic matter. Even in conditions where yields increase, long-term sustainability of production requires maintaining soil health; otherwise, the production system becomes increasingly fragile (Guerra et al., 2020; Nykytiuk et al., 2025).

Moreover**,** increasing CO_2, which is one of the potential reasons for yield increases in some scenarios, can lead to a reduction in the protein content and nutritional quality in the long term, which in turn poses a threat to food security (Marcos-Barbero et al., 2021). Finally, although water productivity (WP) improves by about 17% in future scenarios compared to 2024, this indicator may also be vulnerable to climate fluctuations. Increased temperatures and evaporation can raise the actual water requirement of the plant, and this improvement in WP will not be sustainable if water resources are limited. Overall, although the modeling shows an increase in yield and water productivity, a combination of climatic, biological and soil factors suggests that the sustainability of this trend is not certain and requires adaptive management, cultivar improvement, pest control, and optimal management of water and soil resources (Dehghani et al., 2025; Akhavan Giglou et al., 2023., Basereh et al., 2024).

4. Conclusion

The results of this study showed that climate change will affect temperature, precipitation, evapotranspiration, and ultimately wheat yield and water productivity in Khorasan Razavi Province by 2040. Data analysis shows that the increase in average temperature is more influenced by the increase in minimum temperature. This increase in temperature is especially important in colder stations such as Quchan because it can alter the length of the wheat growth period and plant's water requirement. In terms of precipitation, the results showed that annual precipitation will increase between 11 to 38% in the future. The sustained yield growth indicates that wheat yield in Khorasan Razavi Province will benefit from climate change and increased CO_2. Moreover**,** the increase in atmospheric CO_2 concentration can have positive effects on photosynthesis and biomass production, which is explicitly incorporated into the AquaCrop model.

Overall, although the modeling results indicate that wheat yield and water productivity will increase by 2040, this improvement does not necessarily ensure long-term sustainability of production. Climate change can negatively affect the sustainability of the production system through various pathways, including an increase in pest generations, intensifying plant diseases, the occurrence of heat stresses at critical stages of growth, shifts in the temporal distribution of precipitation, and declines in soil quality. Therefore, the continuation of this increasing trend will only be reliable if it is accompanied by adaptive management, the development of resistant cultivars, improved water and soil management, and integrated pest control. In other words, the increase in yield observed in future scenarios is an opportunity, but without management interventions and climate adaptation, it cannot be considered a sustainable or guaranteed trajectory.

The results obtained can be used as a scientific and practical reference for future planning in the field of water resources management, increasing agricultural productivity, and promoting food security in Iran. Therefore, it is recommended that policymakers and agricultural managers, taking these results into account, develop and implement climate change adaptation strategies at the provincial and national levels to reduce the risks of climate change and capitalize on potential opportunities to increase production and productivity. This study, despite providing valuable results, has several limitations. First, climate and crop yield estimates were based on the output of simulation models, and their accuracy depends on the assumptions and inherent uncertainties of the models. Also, some climate variables such as relative humidity, or wind speed were not simulated in future scenarios. A limitation of the Hargreaves–Samani method is that it does not account for wind speed, humidity, or net radiation, which may also change under future climate conditions and influence ET_0.

Moreover, complex biological processes such as pest population dynamics, crop diseases, and long-term changes in soil quality were not fully represented in the modeling framework. These factors can substantially influence crop growth, stress responses, and ultimately yield sustainability, particularly under future climate conditions where pest outbreaks and disease pressures may intensify. The absence of these biological interactions introduces an additional source of uncertainty, as the model primarily focuses on climatic and physiological drivers of yield. Finally, the results are specific to the environmental characteristics and temporal scope of the study area, and caution is required when extrapolating these findings to other regions with different agro-ecological conditions. Further research incorporating biological stressors and broader spatial scales is recommended to enhance the robustness and generalizability of the conclusions.

Statements and Declarations

Funding

The authors declare that no funds, grants, or other support were received during the preparation of this manuscript.

Data Availability

The data produced in this research are presented in the paper.

Conflict of Interest

The authors of this article declared no conflict of interest regarding the authorship or publication of this article.

Author contributions

Tahmine Dehghani: Data Collection, Data Analysis, Investigation, Methodology, Resources, Software, Writing – original draft, Writing – review and editing; Abdolmajid Liaghat: Conceptualization, Validation, Supervision, Writing – review and editing; Bijan Nazari: Conceptualization, Validation, Supervision, Writing – review and editing.

Declaration of AI Assistance

During the preparation of this work, the authors used the "https://chatgpt.com/" website for editing and language enhancement. The authors have thoroughly reviewed and revised the content as necessary and assume full responsibility for the final manuscript.

Acknowledgment

The authors gratefully acknowledge the Meteorological Organization for supplying the climatic data. This study was carried out as part of the first author’s PhD dissertation, supported by the University of Tehran.

References

1. Aalijahan, M., & Khosravichenar, A. (2021). A multimethod analysis for average annual precipitation mapping in the Khorasan Razavi Province (Northeastern Iran). *Atmosphere*, *12*(5), 592.
2. Ababaei, B., Sohrabi, T., Mirzaei, F., & Karimi, B. (2010). Evaluation of a stochastic weather generator in different climates. *Computer and Information Science*, *3*(3), 217.
3. Abedinpour, M. 2021. The Comparison of DSSAT-CERES and AquaCrop Models for Wheat Under Water–Nitrogen Interactions. *Communications in Soil Science and Plant Analysis*, 52, pp. 2002 - 2017.
4. Afshartabar, R., Mortazavi, S. A., & Khalilian, S. (2023). Evaluation climate change Impact on the production of agricultural products in Marvdasht city. *Iranian Journal of Irrigation & Drainage*, *17*(1), 42-55. (In Persian)
5. Agricultural Yearbook 2022–2023 Field Crops. Planning and Economic Affairs Deputy, Ministry of Agriculture, 2024. In Persian)

6. Ahmadi, M., Etedali, H. R., Salem, A., Al-Mukhtar, M., & Elbeltagi, A. (2024). Simulation of wheat water footprint using AquaCrop model under the climate change, case study in Qazvin plain. *Applied Water Science*, *14*(12), 264.
7. Ahmadpari, H., Khaustov, V., & Amini, A. (2025). Linear Signs and Kendall Lines: Detecting Local Climate Warming through Combined Statistical Approaches. *Nivar, 49*(Special English Issue), 14–33.
8. Akhavan Giglou, K., Kheiry, M., Ahmadpari, H., Abbasi, S. and Kalateh, F. (2023). Investigating virtual water content and physical and economic water productivity indicators in crops (Case study: Moghan irrigation network, Ardabil province). *Water and Soil Management and Modelling, 3*(3), 277-295. (In Persian)
9. Bagheri Khaneghahi, M., HezarJaribi, A., Kamali, M. I., & Zamani, F. (2025). Projection of Temperature and Radiation in Arid and Semi-Arid Climates under Shared Socioeconomic Pathways (SSP) Scenarios. *Water and Soil Management and Modelling*, *5*, 32-48.
10. Bakshi, H. A., Durandish, A., Zarei, N., & Sabohi, M. (2022). Effects of climate change on production yield of major cereals in Iran. *Agricultural Economics*, *16*(2), 27-46.
11. Basereh, F., Ahmadpari, H. and sharifi, M. (2024). Investigating virtual water content and agricultural water productivity indicators in crops (Case study: Dehloran County, Ilam Province). *Water and Soil Management and Modelling*, *4*(3), 1-18. (In Persian)
12. Bouras, E., Jarlan, L., Khabba, S., Er-Raki, S., Dezetter, A., Sghir, F., & Tramblay, Y. (2019). Assessing the impact of global climate changes on irrigated wheat yields and water requirements in a semi-arid environment of Morocco. *Scientific reports*, *9*(1), 19142.
13. Bouteska, A., Sharif, T., Bhuiyan, F., & Abedin, M. (2024). Impacts of the changing climate on agricultural productivity and food security: Evidence from Ethiopia. *Journal of Cleaner Production*.
14. Calanca, P. (2020, May). Underestimation of temperature variability in weather generators and implications for the representation of extreme temperatures in downscaled climate change scenarios. In *EGU General Assembly Conference Abstracts* (p. 4572).
15. Chauhdary, J. N., Li, H., Ragab, R., Rakibuzzaman, M., Khan, A. I., Zhao, J., and Akbar, N. (2024). Climate change impacts on future wheat (Triticum aestivum) yield, growth periods and irrigation requirements: a SALTMED model simulations analysis. *Agronomy*, *14*(7), 1484.
16. Da Conceição, W. N. F., de Faria, R. T., Coelho, A. P., Palaretti, L. F., Dalri, A. B., & de Freitas, E. P. (2024). Calibration, testing and application of the AquaCrop model for bean crop under irrigation regimes. *International Journal of Biometeorology*, *68*(9), 1703-1716.
17. Dastorani, M., Akbari, E., & Qaderi, M. (2025). Investigation of the impact of climate change on runoff in the Kahneh Joghtai watershed using the HadGEM3-GC31-LL model and the SCS curve number method. *Journal of Arid Regions Geographic Studies*, *16*(61), 87-99.
18. Dehghani, T., Liaghat, A, Nazari, B. (2026). Analysis of Climate Scenario Impacts on Irrigated Wheat Water Productivity in Alborz Province Using the AquaCrop Model, Iranian Water Research Journal, (Article in press). (In Persian)
19. Dehghani, T., Nazari, B., Liaghat, A. (2025). Future-oriented agricultural water management with scenario-based evaluation: Case study of Maize in Khuzestan, Special Issue: New Approaches to Water and Soil Management and Modeling, (Article in press). (In Persian)
20. Dehghani, T., Rahimikhoob, A., & Arab, M. (2019). Investigating the effect of Basil planting date on AquaCrop's normalized water productivity. *Iranian Journal of Soil and Water Research*, *49*(6), 1299-1307. (In Persian).
21. Dheyaa, M. A., Al-Mukhtar, M. M., & Shemal, K. (2024). Analyzing the future climate change impacts on meteorological parameters using the LARS-WG model. *Civil Engineering Journal*, *10*(11), 3754-3778.

22. FAO. (2018). AquaCrop Version 6.0: Reference Manual. Food and Agriculture Organization of the United Nations.
23. Fatih, Ü., Kaya, Y. Z., & Mustafa, M. (2020). Daily reference evapotranspiration prediction based on climatic conditions applying different data mining techniques and empirical equations. *Theoretical and applied climatology*, *141*(1-2), 763-773.
24. Fisher, R. A. (1970). Statistical methods for research workers. In *Breakthroughs in statistics: Methodology and distribution* (pp. 66-70). New York, NY: Springer New York.
25. Guerra, C. A., Rosa, I. M., Valentini, E., Wolf, F., Filipponi, F., Karger, D. N., ... & Eisenhauer, N. (2020). Global vulnerability of soil ecosystems to erosion. *Landscape ecology*, *35*(4), 823-842.
26. Hadi, S. H., Alwan, H. H., & Al-Mohammed, F. M. (2024). Analysis of climate change scenarios using the LARS-WG 8 model based on precipitation and temperature trends. *Civil Engineering Journal*, *10*(12), 4019-4042.
27. IPCC (2021b). Sixth Assessment Report (AR6), Working Group II: Impacts, Adaptation, and Vulnerability. Annex I: Global to Regional Atlas Wheat Yield Projections.
28. IPCC, (2021a): Climate Change 2021: The Physical Science Basis. Contribution of Working Group I to the Sixth Assessment Report of the Intergovernmental Panel on Climate Change. [Masson-Delmotte, V., P. Zhai, A. Pirani, S.L. Connors, C. Péan, S. Berger, N. Caud, Y. Chen, L. Goldfarb, M.I. Gomis, M. Huang, K. Leitzell, E. Lonnoy, J.B.R. Matthews, T.K. Maycock, T. Waterfield, O. Yelekçi, R. Yu, and B. Zhou (eds.)]. Cambridge University Press, Cambridge, United Kingdom and New York, NY, USA, 2391 pp.
29. Kavwenje, S., Zhao, L., Chen, L., & Chaima, E. (2022). Projected temperature and precipitation changes using the LARS-WG statistical downscaling model in the Shire River Basin, Malawi. *International Journal of Climatology*, *42*(1), 400-415.
30. Khalili, N., Davary, K., Alizadeh, A., Ansari, H., Rezaee Pazhand, H., Kafi, M., & Ghahraman, B. (2016). Evaluation of the performance of ClimGen and LARS-WG models in generating rainfall and temperature time series in rainfed research station of Sisab, Northern Khorasan. *Water and Soil*, *30*(1), 322-333.
31. Komasi, M., & Doorbashizadeh, B. (2025). Evaluation of fractal theory and LARS-WG downscaling model in precipitation and temperature forecasting via a climate change approach. *Journal of Water and Climate Change*, jwc2025848.
32. Koukouli, P., Georgiou, P., & Karpouzos, D. (2025). Assessment of the Impacts of Climate Change Scenarios on Maize Yield and Irrigation Water Using the CropSyst Model: An Application in Northern Greece. *Agronomy*, *15*(3), 638.
33. Ledolter, J., Gramlich, O. W., & Kardon, R. H. (2020). Parametric statistical inference for comparing means and variances. *Investigative ophthalmology & visual science*, *61*(8), 25-25.
34. Li, Y., Li, N., Javed, T., Pulatov, A. S., & Yang, Q. (2024). Cotton yield responses to climate change and adaptability of sowing date simulated by AquaCrop model. *Industrial Crops and Products*, *212*, 118319.
35. Lotfi, M., Kamali, G. A., Meshkatee, A. H., & Varshavian, V. (2022). Performance analysis of LARS-WG and SDSM downscaling models in simulating temperature and precipitation changes in the West of Iran. *Modeling Earth Systems and Environment*, *8*(4), 4649-4659.
36. Marcos-Barbero, E. L., Pérez, P., Martínez-Carrasco, R., Arellano, J. B., & Morcuende, R. (2021). Genotypic variability on grain yield and grain nutritional quality characteristics of wheat grown under elevated CO2 and high temperature. *Plants*, *10*(6), 1043.
37. Mirosavljević, M., Mikić, S., Župunski, V., Abdelhakim, L., Trkulja, D., Zhou, R., ... & Ottosen, C. O. (2024). Effects of heat stress during anthesis and grain filling stages on some physiological and agronomic traits in diverse wheat genotypes. *Plants*, *13*(15), 2083.

38. Mirshekari, S., Yaghoubi, F., & Hashemi, S. A. (2025). Climate Change Impacts on Wheat Yields in Arid Regions of Iran: A Multimodel Approach for Adaptation Strategies. *International Journal of Plant Production*, 1-16.
39. Naderi, M. (2025). Projections of major climate change indicators over Iran from 2021 to 2080. *Environmental Science and Pollution Research*, 1-23.
40. Najafi, M. R., Abbasian, M., Na, W., RahimiMovaghar, M., Bakhtiari, S., Islam, M. R., ... & Rezvani, R. (2025). Multi-Model Projection of Climate Extremes under 1.5 C–4 C Global Warming Levels across Iran. *International Journal of Climatology*, *45*(4), e8740.
41. Nhemachena, C., Nhamo, L., Matchaya, G., Nhemachena, C. R., Muchara, B., Karuaihe, S. T., & Mpandeli, S. (2020). Climate change impacts on water and agriculture sectors in Southern Africa: Threats and opportunities for sustainable development. *Water, 12*(10), 2673.
42. Nykytiuk, Y., Kravchenko, O., Komorna, O., Bambura, V., & Seredniak, D. (2025). Global climate change will lead to a decrease in the erosion resistance of Polissya and Forest-Steppe soils. *Biosystems Diversity*, *33*(1), e2502-e2502.
43. Obead, I. H., & Hussein, Z. (2024, August). Climate Change Projections in Euphrates River Watersheds in the Middle of Iraq. In *IOP Conference Series: Earth and Environmental Science* (Vol. 1374, No. 1, p. 012046). IOP Publishing.
44. Qi, Y., Zhang, Q., Hu, S., Wang, R., Wang, H., Zhang, K., ... & Yang, Y. (2022). Effects of high temperature and drought stresses on growth and yield of summer maize during grain filling in North China. *Agriculture*, *12*(11), 1948.
45. Raes, D., Steduto, P., Hsiao, T. C., & Fereres, E. (2009). AquaCrop-The FAO crop model to simulate yield response to water. *FAO Land and Water Division, FAO, Rome*.
46. Raoufi, H., & Attayee, S. N. (2025). Assessing Precipitation Trend: a Case Study of Kabul, Afghanistan. *Indonesian Journal of Social and Environmental Issues (IJSEI), 6*(1), 124-134.
47. Raoufi, R. S., & Soufizadeh, S. (2020). Simulation of the impacts of climate change on phenology, growth, and yield of various rice genotypes in humid sub-tropical environments using AquaCrop-Rice. *International Journal of Biometeorology*, *64*(10), 1657-1673.
48. Sedhai, S., Pandey, V. P., Shrestha, M. N., Pradhan, A. M. S., & Shrestha, N. (2023). Climate Change Impact on Water Requirement and Yield of Wheat: An Application of AquaCrop in Madabhar Irrigation Project, Chitwan.
49. Semenov, M. A., & Brooks, R. J. (1999). Spatial interpolation of the LARS-WG stochastic weather generator in Great Britain. *Climate Research*, *11*(2), 137-148.
50. Semenov, M. A., & Stratonovitch, P. (2010). Use of multi-model ensembles from global climate models for assessment of climate change impacts. *Climate research*, *41*, 1-14.
51. Shakoor, A., Shah, S. A., Sattar, M. N., Ogunrinde, A. T., Alharbi, R. S., & Rehman, F. U. (2025). Hydroclimate Drivers and Spatiotemporal Dynamics of Reference Evapotranspiration in a Changing Climate. *Water, 17*(17), 2586.
52. Skendžić, S., Zovko, M., Živković, I. P., Lešić, V., & Lemić, D. (2021). The impact of climate change on agricultural insect pests. *Insects*, *12*(5), 440.
53. Soleymani Nejad, S., Dourandish, A., Sabouhi, M., & Banayan Aval, M. (2019). The effects of climate change on cropping pattern (Case study: Mashhad plain). *Iranian journal of agricultural economics and development research, 50*(2), 249-263. (In Persian)
54. Soltani, A., A. Nahbandani, A. Zeinali, et al. 2019. “Development of an atlas of yield gaps and production potential of major crops in Iran under current and future climate conditions.” Vazhegan Sirang, Tehran. (In Persian)
55. Steduto, P., Hsiao, T. C., & Fereres, E. (2007). On the conservative behavior of biomass water productivity. *Irrigation Science*, *25*(3), 189-207.

56. Steduto, P., Hsiao, T. C., Raes, D., & Fereres, E. (2009). AquaCrop—The FAO crop model to simulate yield response to water: I. Concepts and underlying principles. *Agronomy journal*, *101*(3), 426-437.
57. Stjern, C. W., Samset, B. H., Boucher, O., Iversen, T., Lamarque, J. F., Myhre, G., ... & Takemura, T. (2020). How aerosols and greenhouse gases influence the diurnal temperature range. *Atmospheric Chemistry and Physics*, *20*(21), 13467-13480.
58. Student. (1908). The probable error of a mean. *Biometrika*, 1-25.
59. Suo, X., Jiang, Y., Chen, G., Li, J., Lai, Y., Li, L., ... & Li, B. (2025). Spatial and temporal patterns of precipitation concentration and their associated risks. *Scientific Reports*, *15*(1), 33152.
60. Usta, D. F. B., Teymouri, M., & Chatterjee, U. (2022). Assessment of temperature changes over Iran during the twenty-first century using CMIP6 models under SSP1-26, SSP2-4.5, and SSP5-8.5 scenarios. *Arabian Journal of Geosciences*, *15*(5), 416.
61. Van Bussel, L. G., Grassini, P., Van Wart, J., Wolf, J., Claessens, L., Yang, H., ... & van Ittersum, M. K. (2015). From field to atlas: upscaling of location-specific yield gap estimates. *Field Crops Research*, *177*, 98-108.
62. Wang, K., & Clow, G. D. (2020). The diurnal temperature range in CMIP6 models: climatology, variability, and evolution. *Journal of Climate*, *33*(19), 8261-8279.
63. Wang, Y., Jaworski, C. C., Zi, H., Chen, J., Desneux, N., & Tan, X. (2024). Increased ladybird predation and metabolism do not counterbalance increased field aphid population growth under experimental warming. *Functional Ecology*, *38*(5), 1134-1145.
64. Wilks, D. S. (2011). Statistical methods in the atmospheric sciences (Vol. 100). Academic press.
65. Xiao, D., Li Liu, D., Wang, B., Feng, P., Bai, H., & Tang, J. (2020). Climate change impact on yields and water use of wheat and maize in the North China Plain under future climate change scenarios. *Agricultural Water Management*, *238*, 106238.
66. Xu, Y., Li, T., Xu, M., Tan, L., & Shen, S. (2024). Assessing climate change effects on winter wheat production in the 3H plain: insights from bias-corrected CMIP6 projections. *Agriculture*, *14*(3), 469.
67. Ye, Z., Qiu, X., Chen, J., Cammarano, D., Ge, Z., Ruane, A. C., ... & Zhu, Y. (2020). Impacts of 1.5 C and 2.0 C global warming above pre-industrial on potential winter wheat production of China. *European Journal of Agronomy*, *120*, 126149.
68. Zare, M., Azam, S., Sauchyn, D., & Yaghoubi, F. (2025). Assessment and mapping of climate change impacts on spring wheat yield in Southern Saskatchewan using DSSAT and high-resolution RCM projections. *Scientific Reports*, *15*(1), 33680.
69. Zeinali Mobarakeh, Z., Deihimfard, R., & Kambouzia, J. (2018). Modelling the Impacts of Climate Change on Irrigated Wheat Yield Under Water Limited Conditions in Khorasan Razavi Province. Journal of Agricultural science and sustainable production, 28(3), 155-169. (In Persian)
70. Zeinali Mobarakeh, Z., Deihimfard, R., & Kambouzia, J. (2019). Evaluation of climate change effects and adaptation strategies on grain yield and water use efficiency of irrigated wheat (Triticum aestivum): A cae study in Khorasan Razavi province. *Journal of Plant Production Research*, *26*(3), 71-87. (In Persian)
71. Zenozi Alamdari, N., Sobhani, B., Eshahi, M., & Mohammadi, M. (2025). Precipitation and temperature zoning of Khorasan Razavi province using data from the sixth climate change report (CMIP6). *Journal of Environmental Science Studies*, *9*(4), 9761-9753.
72. Zynal Zadeh, M., Gobadijanbaz, G., Motevalli, S., Taherian, M., & Kouhi, M. (2025). Projecting the changes of extreme climate indices in Razavi Khorasan province (Case study: Torbat Heydarieh and Kashmar). *Journal of Climate Research*, *1403*(59), 47-60.